JOURNAL OF COMPUTATIONAL PHYSICS 37, 399–421 (1980)

The Effect of Cell Reynolds Number on the Computation of a Boundary Layer*

G. W. HEDSTROM AND ALBERT OSTERHELD†

University of California, Lawrence Livermore Laboratory, Livermore, California 94550

Received April 25, 1979; revised November 20, 1979

We carefully analyze the behavior of a numerical solution of the linearized Navier–Stokes equations in a problem with a boundary layer. We show that the effect of discretization is to increase the viscosity and that oscillations arise only if bad outflow boundary conditions are used. Computations show the same effects for the full Navier–Stokes equations.

1. INTRODUCTION

In this paper we determine the accuracy of the computation of a 2-dimensional flow with a boundary layer. In particular, we find the solution of the differential equation

$$u_x = \nu(u_{xx} + u_{yy}) \tag{1.1}$$

on the quarter plane $x > 0$, $y > 0$ with boundary conditions

$$\begin{aligned} u(x, 0) &= 0, \qquad u(0, y) = 1 \\ u(x, y) &\text{ bounded as } |x| + |y| \to \infty. \end{aligned} \tag{1.2}$$

Then we compare u with the solution of the difference equation

$$\begin{aligned} (u_h(x + h, y) - u_h(x - h, y))/(2h) = \nu(&u_h(x + h, y) + u_h(x, y + h) \\ &+ u_h(x - h, y) + u_h(x, y - h) \\ &- 4u_h(x, y))/h^2 \end{aligned} \tag{1.3}$$

with the same boundary conditions (1.2). We are interested in the case when ν is a small positive number. Thus, the solution u of (1.1) and (1.2) is nearly equal to 1 ex-

* This work was performed under the auspices of the U.S. Department of Energy by the Lawrence Livermore Laboratory under contract number W-7405-ENG-48.

† Currently a graduate student in the Department of Physics, Stanford University, Stanford, Calif. 94305.

0021-9991/80/120399–23$02.00/0

581/37/3-8

cept in a boundary layer near the x-axis [8]. The cell Reynolds number [10] for (1.3) is $R_c = uh/v$, but our formulas are simpler if expressed in terms of the parameter

$$\beta = h/(2v), \tag{1.4}$$

which we shall call the half cell Reynolds number.

In 1-dimensional flow it is known [10, pp. 161–165] that if there is a boundary layer and if $\beta > 1$, then the solution of (1.3) has oscillations. This effect is small for β near 1, and it becomes more pronounced as β increases. In two dimensions this case corresponds to the presence of a boundary layer perpendicular to the flow. In our case, (1.1) and (1.2), the boundary layer is parallel to the flow, and we find no oscillations of any consequence for any value of β. The theory does predict the presence of highly damped oscillations near the inlet if $\beta > 1$, but they are not visible in our computations. Our conclusion is that for u from (1.1) and (1.2) and u_h from (1.2) and (1.3) and for any $\beta > 1$ the difference $u - u_h$ is very small except in the boundary layer.

The effect of β is most clearly seen in the asymptotic behavior of u and u_h. Theorem 2.1 includes the result that as $x/v \to \infty$ and $y/x \to 0$ we have

$$u(x, y) \sim \operatorname{erf}\{y2^{-1}(vx)^{-1/2}(1 - y^2/(8x^2) + O(y^4/x^4))\}. \tag{1.5}$$

Theorem 3.1 implies that as $x/h \to \infty$, $y/x \to 0$, and $\beta y/x \to 0$ we have

$$u_h(x, y) \sim \operatorname{erf}\{y2^{-1}(vx)^{-1/2}(1 - (3 + \beta^2)y^2/(24x^2) + O(y^4/x^4))\}. \tag{1.6}$$

Thus, the width of the boundary layer for u_h increases as the half cell Reynolds number β increases.

We remark that we also obtain (1.6) if we use the methods of Section 3 to find the behavior in the boundary layer ($x/v \to \infty$, $y/x \to 0$, $\beta y/x \to 0$) of the solution of

$$u_x = vu_{yy} + v(1 + \beta^2/3)u_{xx}$$

with boundary conditions (1.2). Thus, we have obtained a model partial differential equation for (1.3), and it shows that the effect of the discretization is an increase in viscosity. We may also obtain this model equation by a perturbation argument, as follows. A Taylor series expansion of (1.3) gives

$$u_x + (h^2/6)u_{xxx} + \cdots = v(u_{xx} + u_{yy} + (h^2/12)(u_{xxxx} + u_{yyyy}) + \cdots).$$

If we set $y = v^{1/2}z$, we obtain the simpler equation

$$u_x = u_{zz} + v(u_{xx} + (\beta^2/3)u_{zzzz}) + O(v^2)$$

as $v \to 0$ with β bounded. If we use $u_{xx} = u_{zzzz} + O(v)$, drop the $O(v^2)$ terms, and transform back to (x, y)-coordinates, we obtain our model equation.

We can apply a similar argument to the upstream difference approximation. That is the difference scheme with the same right-hand side as (1.3) but with left-hand side

$$(u_h(x, y) - u_h(x - h, y)/h.$$

A Taylor series argument yields the model equation

$$u_x = \nu u_{yy} + \nu(1 + \beta + \beta^2/3)u_{xx}.$$

Again, we see that the discretization increases the effective viscosity.

The model equation does not tell the whole story, though, because the solution of (1.3) actually contains two components, one completely spurious and the other modeled by the model equation. The boundedness required by (1.2) eliminates this spurious component for the problem on the full quarter plane, but, of course, we compute on bounded regions. The spurious component is more noticeable when $\beta > 1$, because then it is oscillatory. The elimination of this spurious component on a bounded domain requires the use of an outflow boundary condition. In Section 4 we use the ideas of Engquist and Majda [6] to show that the exact outflow condition is in terms of a pseudodifferential operator, and there are difference approximations to it. Our first and second approximate outflow boundary conditions are discretizations of

$$u_x = 0 \tag{1.7}$$

and

$$u_x = \nu u_{yy}. \tag{1.8}$$

It is not so surprising that these are good outflow conditions, and (1.7) is one of the outflow conditions recommended by Roache [10, p. 165]. In our computations in Section 5, we see little difference between the results of using discretizations of (1.7) and (1.8).

We remark that in this paper we have emphasized the behavior of u_h for large cell Reynolds number ($\beta > 1$). Thus, our work differs from that of Bramble, Hubbard, and Thomée [2] and Sapagovas and Skirmantas [12], for they show that $u - u_h$ is small if both h and β are sufficiently small.

Finally, we remark that our reason for studying (1.1) in such detail is that it is a linearization of the Navier–Stokes equations

$$\begin{aligned} uu_x + vu_y + p_x &= \nu(u_{xx} + u_{yy}), \\ uv_x + vv_y + p_y &= \nu(v_{xx} + v_{yy}), \\ u_x + v_y &= 0. \end{aligned} \tag{1.9}$$

In Section 5 we present results of numerical experiments with a central difference scheme for (1.9). We find that here also there are no significant oscillations if the main flow is parallel to both the boundary layer and to grid lines and if proper outflow boundary conditions based on (1.8) are used.

2. Asymptoric Behavior of u

In this section we represent the solution u of (1.1) and (1.2) as a Fourier integral. The integrand has a pole at the origin and a saddle point whose location depends upon a parameter. The boundary layer near the x-axis corresponds to the coalescence of the saddle point with the pole. The classical saddle-point method of Laplace is not applicable in this situation; we use, instead, a combination of the methods of Bleistein [1] and van der Waerden [13] to obtain an asymptotic expansion for u.

If we continue u across the x-axis as an odd function in y and solve problem (1.1) and (1.2) using a Fourier transform in y, we find after a change of variable that

$$u(x, y) = \int_{-\infty}^{\infty} (i\pi\theta)^{-1} \exp\{p\phi(\theta)\}\, d\theta, \tag{2.1}$$

where the integral is a Cauchy principal value and $p = x/(2v)$, $\omega = y/x$, and

$$\phi(\theta) = 1 - (1 + \theta^2)^{1/2} + i\omega\theta.$$

The integral (2.1) may be evaluated explicitly, but we postpone doing that to Section 5. Our aim here is to illustrate a method for finding the asymptotic behavior of u in the boundary layer. It is easy to verify that the integral (2.1) does indeed solve problem (2.1) and (2.2).

Let us say a few words about ϕ. The saddle point, that is, the point where $\phi' = 0$, is given by

$$\theta_0 = i\omega(1 + \omega^2)^{-1/2}.$$

We wish to extend ϕ to complex values of θ, so we take the branch such that $(1 + \theta^2)^{1/2} > 0$ for θ real, and we cut the θ-plane on the imaginary axis from i to $i\infty$ and from $-i$ to $-i\infty$. Thus, in place of the real line we may integrate along the line $\gamma = \{\theta: \operatorname{Im}\theta = \operatorname{Im}\theta_0\}$, provided that we add to the integral the contribution from the residue at the pole. In other words, we add 1 to the integral when we move the path into the upper half of the θ-plane. Since θ_0 is on the imaginary axis, it is easy to see that on γ the elevation $\operatorname{Re}\phi(\theta)$ takes its maximum value at $\theta = \theta_0$.

Suppose we try the saddle-point method of Laplace, just to see how well it works. Note two danger signals: As $\omega \to \infty$, we have $\theta_0 \to i$, but i is a branch point. Also, as $\omega \to 0^+$, we have $\theta_0 \to 0$, but 0 is a pole. Thus, we may use the ordinary saddle-point method only under restrictions of the form

$$0 < \omega_0 \leqslant \omega \leqslant \omega_1 < \infty, \tag{2.2}$$

and it yields [9, pp. 125–127]

$$u(x, y) = 1 - \exp\{p(1 - (1 + \omega^2)^{1/2})\}(2^{1/2}(\pi p)^{-1/2}\omega^{-1}(1 + \omega^2)^{-1/4} + O(p^{-3/2})) \tag{2.3}$$

as $p = x/(2v) \to \infty$ with $\omega = y/x$ as in (2.2).

Relation (2.3) is not very interesting because it says only that u is close to 1 when p is large and when (x, y) is in a sector (2.2). Actually, we care more about the nature of u in the transition region $0 \leqslant \omega \leqslant \omega_0$. It is also clear that we do not get $u \to 0$, as we should, if we let $\omega \to 0$ in the main terms of (2.3). The cause of the difficulty is our careless treatment of the pole. By being more careful, we obtain the following result.

THEOREM 2.1. *Let u be the solution of* (1.1) *and* (1.2), *and let* $\omega = y/x$, $p = x/(2\nu)$, *and*

$$A(\omega) = 2^{1/2}((1 + \omega^2)^{1/2} - 1)^{1/2}. \tag{2.4}$$

Then for any positive ω_1 and for $0 \leqslant \omega \leqslant \omega_1$ and $p \to \infty$ we have

$$u(x, y) = \operatorname{erf}\{A(p/2)^{1/2}\} + \exp\{-pA^2/2\}\,(B(\omega)p^{-1/2} + O(p^{-3/2})), \tag{2.5}$$

$$B(\omega) = (2/\pi)^{1/2}(A^{-1} - \omega^{-1}(1 + \omega^2)^{-1/4}), \tag{2.6}$$

where $O(p^{-3/2})$ is uniform in ω.

Remarks. It follows from (2.4) that

$$A(\omega) = \omega - \omega^3/8 + O(\omega^5), \qquad \omega \to 0.$$

Hence, $B(\omega) = O(\omega)$ as $\omega \to 0$, and (1.5) follows from (2.5). We can also show that (2.5) reduces to (2.3) as $p \to \infty$ with condition (2.2). In fact, this follows directly from (2.5), (2.6), and the expansion for the error function [9, p. 67]

$$\operatorname{erf}\{z\} = 1 - \pi^{-1/2}z^{-1}\exp\{-z^2\}\,(1 + O(z^{-1})), \qquad z \to \infty.$$

Proof of the theorem. We use a combination of a transformation of Bleistein [1] and the treatment of poles of van der Waerden [13]. Bleistein's transformation

$$\phi(\theta) = -\xi^2/2 + iA(\omega)\xi \tag{2.7}$$

takes the integral (2.1) to the standard form

$$u(x, y) = \int_{-\infty}^{\infty} (\pi i\xi)^{-1}\, g(\xi)\exp\{-p(\xi^2/2 - iA\xi)\}\, d\xi \tag{2.8}$$

with $g(\xi) = (\xi/\theta)\, d\theta/d\xi$. Again, the integral is a principal value, and we have deformed the path of integration. The value of $A(\omega)$ is chosen so that

$$d\theta/d\xi = -(\xi - iA)/\phi'(\theta)$$

is nonsingular at $\theta = \theta_0$. Hence, $\theta = \theta_0$ maps into $\xi = iA$, giving (2.4).

The van der Waerden [13] method of treating the pole in (2.8) is to write

$$g(\xi)/\xi = 1/\xi + \sum_0^\infty c_j(\xi - iA)^j$$

and to integrate formally, termwise. We show in the Appendix that $g(\xi)$ is analytic in a strip which allows us to replace the path of integration in (2.8) by the line Im $\xi = A$. Thus, we get

$$u(x, y) = \operatorname{erf}\{A(p/2)^{1/2}\} + \exp\{-pA^2/2\} \sum_0^\infty c_{2j}(\pi i)^{-1}\Gamma(j + 1/2)(2/p)^{j+1/2}. \tag{2.9}$$

Because (2.9) is a classical saddle-point expansion, we conclude from the general theory [9, p. 127] that (2.5) follows from (2.9) with

$$B = 2^{1/2}\Gamma(1/2)\, c_0/\pi i. \tag{2.10}$$

The value (2.6) of B is obtained by finding c_0. Details are given in the Appendix.

3. Asymptotic Behavior of u_h

We now repeat the above analysis for the solution u_h of problem (1.2) and (1.3). For problem (1.1) and (1.2) we saw in Theorem 2.1 that there are two natural parameters, ω and p. For problem (1.2) and (1.3) there is an additional parameter h, and this complicates the analysis. The plan of this section is as follows. We first represent u_h as a Fourier integral. We then prove two lemmas which describe the topography of the integrand in the complex plane. Then the section ends with a theorem on the asymptotic behavior of u_h.

We begin by extending u_h as an odd function in y and taking the discrete Fourier transform in y,

$$\tilde{u}_h(x, \theta) = \sum_{-\infty}^{\infty} u_h(x, y_k)e^{-ik\theta}, \qquad y_k = kh.$$

Note that in this setting the Fourier inversion formula is

$$u_h(x, y_k) = (2\pi)^{-1}\int_{-\pi}^{\pi} \tilde{u}_h(x, \theta)e^{ik\theta}\, d\theta. \tag{3.1}$$

The discrete Fourier transform of (1.3) is

$$\beta(\tilde{u}_h(x + h, \theta) - \tilde{u}_h(x - h, \theta)) = \tilde{u}_h(x + h, \theta) - 2s\tilde{u}_h(x, \theta) + \tilde{u}_h(x - h, \theta), \tag{3.2}$$

where

$$s(\theta) = 2 - \cos\theta \tag{3.3}$$

and β is half the cell Reynolds number, as in (1.4). If $\beta = 1$, the solution of (3.2) at $x_n = nh$ is

$$\tilde{u}_h(x_n, \theta) = b_1(\theta) r_1^n$$

for arbitrary b_1 and for $r_1 = 1/s(\theta)$. If $\beta \neq 1$ and $\beta > 0$, the solution of (3.2) has two arbitrary functions $b_1(\theta)$ and $b_2(\theta)$, and we have

$$\tilde{u}_h(x_n, \theta) = b_1 r_1^n + b_2 r_2^n$$

with

$$r_m = (-s - (-1)^m (s^2 + \beta^2 - 1)^{1/2})/(\beta - 1), \qquad m = 1, 2. \tag{3.4}$$

For real θ we have $|r_2| > 1$ and $|r_1| \leqslant 1$, so that the $\tilde{u}_h$ determined by (1.2) is

$$\tilde{u}_h(x_n, \theta) = -i \cot(\theta/2)\, r_1^n. \tag{3.5}$$

Note that (3.5) is also valid when $\beta = 1$. Note also that the spurious component $b_2 r_2^n$ simply drops out of this problem.

We obtain the Fourier representation of u_h by substituting (3.5) into (3.1),

$$\begin{aligned} u_h(x_n, y_k) &= (2\pi i)^{-1} \int_{-\pi}^{\pi} \cot(\theta/2) \exp\{n(\log r_1(\theta) + i\omega\theta)\}\, d\theta, \\ \omega &= k/n = y_k/x_n. \end{aligned} \tag{3.6}$$

The function $\log r_1(\theta)$ is well defined and real because $r_1(\theta) > 0$ for real θ. In the Appendix we construct a domain Ω in the strip $-\pi \leqslant \operatorname{Re}\theta \leqslant \pi$, $\operatorname{Im}\theta \geqslant 0$ such that

$$\phi_h(\theta) = \log r_1(\theta) + i\omega\theta \tag{3.7}$$

is analytic on Ω. This involves the removal of one branch cut if $0 < \beta < 1$ and two branch cuts if $\beta > 1$. The case $\beta > 1$ is shown in Fig. 1.

The saddle points of ϕ_h are the solutions of $\phi_h' = 0$, that is, θ_0 such that

$$\sin\theta_0 = i\omega(\beta^2 + s_0^2 - 1)^{1/2}, \qquad s_0 = 2 - \cos\theta_0. \tag{3.8}$$

Upon squaring (3.8), solving for s_0, and deleting extraneous roots, we find that there is at least one saddle point θ_0 in Ω,

$$\begin{aligned} s_0 &= (2 - ((1 + \omega^2)^2 + \beta^2\omega^2(1 - \omega^2))^{1/2})/(1 - \omega^2), && \omega \neq 1, \\ s_0 &= 1 - \beta^2/4, && \omega = 1. \end{aligned} \tag{3.9}$$

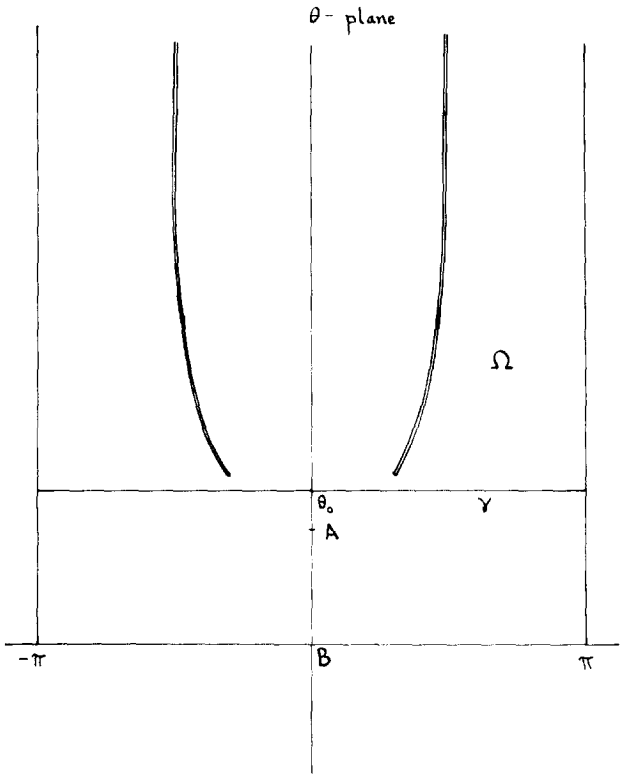

FIG. 1. θ-plane.

If s_0 is real, we see that $s_0 < 1$, so that θ_0 (from $\cos \theta_0 = 2 - s_0$) is imaginary. We integrate along the path as in Fig. 1,

$$\gamma = \{\theta: -\pi < \operatorname{Re} \theta < \pi, \operatorname{Im} \theta = \operatorname{Im} \theta_0\}.$$

It is convenient to restrict somewhat the range of parameters $0 < \beta < \infty$, $0 < \omega < \infty$. The case $\beta \to 0$ has already been treated in [2, 12], so we shall take $\beta \geqslant \beta_0 > 0$. (Actually, we could include $\beta \to 0$ if we were to use a different set of parameters.) If $\beta > 1$ and ω is too large, the path of integration γ crosses the branch cuts. This is actually only a minor technicality, but for the moment we restrict ω to avoid its occurrence. In Lemma A2 (in the Appendix) we show the existence of a function $P(\beta)$ such that for $0 < \omega < P(\beta)$ the path γ does not cross the branch cuts. We also show there that $P(\beta)$ is bounded away from zero, so that the sector $0 \leqslant \omega \leqslant P(\beta)$ contains the boundary layer.

Under these restrictions we have the following characterization of the asymptotic behavior of u_h.

THEOREM 3.1. *Let u_h be the solution of* (1.2) *and* (1.3), *and let* $\omega = y/x$, $n = x/h$, *and* $\beta = h/(2\nu)$ *with* n *and* y/h *integers. Let* β_0 *be any positive number, and let* $\beta \geqslant \beta_0$ *and* $P(\beta)$ *as given by Lemma A*2. *Let* θ_0 *be the saddle point in* Ω *given by* (3.9), *and let*

$$A = (-2\phi_h(\theta_0))^{1/2}, \tag{3.10}$$

$$c_0 = 2(-\phi_h''(\theta_0))^{-1/2}\cot(\theta_0/2) + i/A. \tag{3.11}$$

Then for $0 \leqslant \omega \leqslant \min(\omega_3, P(\beta))$, ω_3 *any positive number, and for* $n \to \infty$ *we have*

$$u_h(x, y) = \operatorname{erf}\{(-n\phi_h(\theta_0))^{1/2}\} + n^{-1/2}\exp\{n\phi_h(\theta_0)\}\,(-ic_0(2/\pi)^{1/2} + O(n^{-1})). \tag{3.12}$$

Remarks. By making Taylor expansions which are valid as $\omega \to 0$ and $\beta\omega \to 0$, we easily obtain (1.6) from (3.12). Note that $n = x/h$ plays the role in Theorem 3.1 which $p = x/(2\nu)$ plays in Theorem 2.1. In fact, p is the natural parameter for (1.1), while n and β are the natural parameters for (1.3).

Proof. Because $n\omega$ is an integer, the integrand in (3.6) is periodic. Thus, we may deform the contour from the segment $(-\pi, \pi)$ to the line γ through θ_0. In doing so, we must add 1 in order to account for the residue from the pole at the origin. As in the proof of Theorem 2.1 we make the Bleistein transformation [1],

$$\phi_h(\theta) = -\xi^2/2 + iA\xi,$$

with A chosen so that the saddle point θ_0 maps into the saddle point $\xi = iA$ and with the branch chosen so that $\theta = 0$ maps into $\xi = 0$. Thus, A is required to be as in (3.10). The result of these changes is the representation

$$u_h(x, y) = 1 + \int_{\gamma_\eta'} (\pi i\xi)^{-1} g(\xi)\exp\{-n(\xi^2/2 - iA\xi)\}\,d\xi, \tag{3.13}$$

where γ_η' is the image of γ_η in the ξ-plane and

$$g(\xi) = 2\xi\cot(\theta/2)\,d\theta/d\xi.$$

As in Section 2 we see that the function $g(\xi)$ is analytic at both $\xi = 0$ and $\xi = iA$. Hence, following van der Waerden [13], we may set

$$g(\xi)/\xi = 1/\xi + \sum_0^\infty c_j(\xi - iA)^j. \tag{3.14}$$

We obtain (3.11) from the equation

$$c_0 = (g(iA) - 1)/(iA),$$

together with a Taylor series for $\xi(\theta)$ about $\theta = \theta_0$. Upon inserting (3.14) into (3.13), we obtain the asymptotic series

$$u_h(x, y) = \operatorname{erf}\{A(n/2)^{1/2}\} + \exp\{-nA^2/2\} \sum_0^\infty c_{2j}(\pi i)^{-1} \Gamma(j + \tfrac{1}{2})(2/n)^{j+1/2}.$$

The relation (3.12) now follows immediately, proving the theorem.

We close this section with a few remarks about the behavior of $u_h(x, y)$ for $n \to \infty$ with $\beta > 1$ and $\omega > P(\beta)$. A detailed description would require the consideration of the contribution from making detours around the branch points and from the effect of the coalescence of two saddle points as $\omega \to \omega_1$ (from (A4)). The oscillations mentioned in the Introduction arise from these effects. At the very least, we would like to estimate $|u_h - 1|$ outside the boundary layer and show that these effects are very small. In the Appendix we show that $|u_h - 1|$ is even smaller for $\omega > P(\beta)$ than it is for $\omega = P(\beta)$. (Note that Theorem 3.1 gives us an estimate of the size of $|u_h - 1|$ for $\omega = P(\beta)$.)

4. Outflow Boundary Conditions

In this section we determine the effect of truncating the domain and imposing various boundary conditions at the outflow. The numerical significance of this effect is obvious, for we must restrict the size of the region on which we compute. Let v_h be the solution of the difference equation (1.3) on the strip

$$\{(x_n, y_k): n = 0,1,..., N; \quad k = 0, 1, 2,...\},$$

subject to the boundary conditions

$$\begin{aligned} &v_h(x_n, 0) = 0 \qquad (n = 0, 1,..., N), \\ &v_h(0, y_k) = 1 \qquad (k = 1, 2,...), \\ &v_h(x_n, y_k) \text{ is bounded as } k \to \infty. \end{aligned} \tag{4.1}$$

We do not truncate the problem at some $k = K$ because the effect of doing so is, at worst, the introduction of a boundary layer at $y = y_K$ like the one at $y = 0$.

Let us discuss possible conditions at the outflow $x = x_N$. We shall see that the best condition at the outflow is in terms of a pseudodifferential operator as in [6], and we give two difference approximations to it. The motivation is as follows. Suppose we extend v_h as an odd function of y. Then the general solution of (1.3) satisfying (4.1) has discrete Fourier transform

$$\tilde{v}_h(x_n, \theta) = b_1 r_1^n + b_2 r_2^n, \tag{4.2}$$

where r_1 and r_2 are given by (3.4) and

$$b_1(\theta) + b_2(\theta) = -i\cot(\theta/2). \tag{4.3}$$

(If $\beta = 1$, set $b_2 r_2^n = 0$.) Thus, it is clear that $\tilde{v}_h$ is a truncation of $\tilde{u}_h$ (given by (3.6)) to a smaller domain if and only if $b_2 = 0$. This situation is realized if and only if

$$\tilde{v}_h(x_N, \theta) = r_1 \tilde{v}_h(x_{N-1}, \theta).$$

Because r_1 is not a quotient of trigonometric polynomials, this exact outflow condition cannot be written in terms of differences of v_h. However, if we approximate $r_1(\theta)$ by a quotient of trigonometric polynomials $f(\theta)$, then the condition

$$\tilde{v}_h(_N, \theta) = f(\theta)\, \tilde{v}_h(x_{N-1}, \theta) \tag{4.4}$$

corresponds to an approximate outflow condition.

In order to get some idea in what sense f should approximate r_1, we first find the values of b_1 and b_2 determined by (4.2)–(4.4),

$$b_1 = i\cot(\theta/2)/(1 - Q),$$
$$b_2 = -i\cot(\theta/2)Q/(1 - Q),$$
$$Q = (f - r_1)(f - r_2)^{-1}(r_1/r_2)^{N-1}.$$

Thus, it follows that

$$\tilde{u}_h - \tilde{v}_h = -i\cot(\theta/2)\, Q(1 - Q)^{-1}(r_1^n - r_2^n). \tag{4.5}$$

In view of the role of the pole of $\cot(\theta/2)$ in generating the boundary layer in Section 3, it seems desirable at least to choose f so that $Q\cot(\theta/2)$ is regular at the origin. In fact, we shall see in Theorem 4.2 that the condition $f(0) \neq r_1(0)$ gives the oscillations discussed by Roache [10], and we shall see in Theorem 4.1 that we should choose f so as to make $|r_1(\theta) - f(\theta)|$ small as $\theta \to 0$.

It follows from (3.5) that

$$r_1(\theta) = 1 - \theta^2/(2\beta) + O(\theta^4), \qquad \theta \to 0,$$

so that we might take

$$f(\theta) = 1 \tag{4.6}$$

or perhaps

$$1/f(\theta) = 1 + (1 - \cos\theta)/\beta. \tag{4.7}$$

Condition (4.6) corresponds to

$$u_h(x_N, y_k) = u_h(x_{N-1}, y_k), \tag{4.8}$$

while (4.7) corresponds to

$$u_h(x_{N-1}, y_k) = u_h(x_N, y_k) - (2\beta)^{-1}\,(u_h(x_N, y_{k-1}) - 2u_h(x_N, y_k) + u_h(x_N, y_{k+1})). \tag{4.9}$$

It is clear that (4.8) is a discretization of (1.7) and (4.9) a discretization of (1.8).

We now give the theorem on good outflow boundary conditions.

THEOREM 4.1. *Let f be a quotient of trigonometric polynomials such that in a strip*

$$R = \{\theta: 0 \leqslant \operatorname{Im}\theta < \eta_1, \eta_1 \leqslant \operatorname{Im}\theta_b\},$$

f is analytic, and $|Q(\theta)| \leqslant 1/2$. For some positive integer q and some constant $C_1 \neq 0$ let

$$f(\theta) = r_1(\theta) + C_1\theta^q + O(|\theta|^{q+1}), \qquad \theta \to 0.$$

$\omega = y_k/(2x_N - x_n)$. Then there exist positive constants D and C_j $(j = 2, 3, 4, 5)$ such that

$$|u_h(x_n, y_k) - v_h(x_n, y_k)| \leqslant C_2(\beta\omega)^{q-1}\beta^{1/2}m^{-1/2}\exp\{-C_3 m\beta\omega^2\} \tag{4.10}$$

if $\beta\omega \leqslant D$ and

$$|u_h(x_n, y_k) - v_h(x_n, y_k)| \leqslant C_4\exp\{-C_5 m\omega\}, \qquad \beta\omega > D. \tag{4.11}$$

Remark. For boundary condition (4.8) we have $q = 2$, and for (4.9) we have $q = 4$. In both cases the required strip exists.

Proof. Because of the identity $r_1 r_2 = (1+\beta)/(1-\beta)$, we may write (4.5) in the form

$$\begin{aligned} \tilde{u}_h - \tilde{v}_h &= -iG(\theta)\alpha^{N-1}\,(r_1^{2N+n-2} - \alpha^{-n}r_1^{2N-n-2}), \\ G(\theta) &= \cot(\theta/2)(f - r_1)(f - r_2)^{-1}\,(1 - Q)^{-1}, \\ \alpha &= (1-\beta)/(1+\beta). \end{aligned} \tag{4.12}$$

Thus, the proof of the theorem is reduced to an estimate of the inverse Fourier transform

$$w(x_n, y_k) = (2\pi i)^{-1}\int_{-\pi}^{\pi} G(\theta)\exp\{m(\log r_1(\theta) + i\omega\theta)\}\,d\theta \tag{4.13}$$

for $m = 2N \pm n - 2$ and $\omega = k/m$. The exponential factor in (4.13) is the same as that in (3.6), and again we set $\phi_h(\theta) = \log r_1(\theta) + i\omega\theta$. The conditions on f guarantee that

G is holomorphic in R, so that the main difference between (4.13) and (3.6) is that (3.6) has a pole and (4.13) does not. If $\beta\omega$ is small enough so that the saddle point θ_0 is in R, we deform the path in (4.13) to the path γ_η of (A7) through θ_0. Thus, we may use the standard saddle-point method [9, p. 127] to show that for $m \to \infty$ and $\beta\omega \leqslant D$ we have

$$w = -iG(\theta_0)(2m\pi\,|\phi_h''(\theta_0)|)^{-1/2} \exp\{m\phi_h(\theta_0)\}\,(1 + O(m^{-1})).$$

Since by (3.10) we have $\theta_0 = i\beta\omega + O(\beta^3\omega^3)$ as $\beta\omega \to 0$, it follows that for $\beta\omega \leqslant D$ we have $\phi_h(\theta_0) \leqslant -C_3\beta\omega^2$ and $|\phi_h''(\theta_0)| \geqslant C\beta$ for some positive C. This proves (4.10). For $\beta\omega > D$ the proof of (4.11) is the same as the proof of (A14).

In Theorem 4.2 we see the bad effect of choosing f in (4.4) so that $f(0) \neq 1$. The most important special case is $f = 0$, which gives $v_h(x_N, y_k) = 0$.

THEOREM 4.2. *Let f be a quotient of trigonometric polynomials such that $f(0) \neq 1$ and such that in a strip*

$$R = \{\theta: 0 \leqslant \operatorname{Im}\theta \leqslant \eta_1,\ \eta_1 \leqslant \operatorname{Im}\theta_b\}$$

f is analytic and $|Q(\theta)| \leqslant 1/2$. For some positive β_0 let $\beta \geqslant \beta_0$, let $\alpha = (1-\beta)/(1+\beta)$, and let

$$\lambda = (f(0) - 1)(f(0) - 1/\alpha)^{-1}\,(1 - \alpha^{N-1}(f(0) - 1)/(f(0) - 1/\alpha))^{-1}.$$

Furthermore, let $m_j = 2N - 2 + (-1)^j n$ and $\omega_j = k/m_j$. Then as $m_1 \to \infty$ and $\beta\omega_1 \to 0$ we have

$$u_h(x_n, y_k) - v_h(x_n, y_k) \sim \lambda\alpha^{N-1}\,(\alpha^{-n}\operatorname{erf}\{\omega_1(m_1\beta/2)^{1/2}\} - \operatorname{erf}\{\omega_2(m_2\beta/2)^{1/2}\}).$$

Remarks. We see that under the conditions of Theorem 4.2 the difference $u_h - v_h$ has a boundary layer near the x-axis. Furthermore, since $\alpha < 0$ for $\beta > 1$, the term $\alpha^{-n}\operatorname{erf}\{\ldots\}$ gives rise to grid-sized oscillations. Also, as in (A14) if $\beta\omega > D$, we have

$$|u_h - v_h - \lambda\alpha^{N-1}(\alpha^{-n} - 1)| \leqslant C\lambda\alpha^{N-1}(\alpha^{-n} + 1)\exp\{-C'm_1\omega_1\}.$$

This is the 1-dimensional effect [10].

Proof. As in the proof of Theorem 4.1, we use the representation (4.12) to reduce the problem to one of estimating the integral (4.13). This time, however, $G(\theta)$ has a pole at the origin with residue 2λ. But we saw how to treat a pole in the proof of Theorem 3.1, and the argument used there shows that

$$w \sim \lambda\operatorname{erf}\{\omega(m\beta/2)^{1/2}\,(1 + O(\beta^2\omega^2))\}$$

as $m \to \infty$ and $\beta\omega \to 0$. This proves the theorem.

5. Numerical Examples

In this section we report on some computations which illustrate Theorems 4.1 and 4.2. We also show computations for the Navier–Stokes equations (1.9). We begin with the linear problem (1.3).

One advantage of studying (1.1) and (1.2) is that an explicit solution is known. In fact, from (2.1) and a table of transforms [7, p. 16, formula (26)] we find that the solution of (1.1) and (1.2) is

$$u(x, y) = x(\nu\pi)^{-1} \exp\{x/(2\nu)\} \int_0^y (x^2 + z^2)^{1/2} K_1 \{(2\nu)^{-1}(x^2 + z^2)^{1/2}\}\, dz, \quad (5.1)$$

where K_1 is the modified Bessel function of order 1. In our computations for (1.3) we arbitrarily chose a grid of size 16×28. The mesh size h is arbitrary, and $\beta = h/(2\nu)$ is the relevant parameter. We chose $h = 1$ for convenience. We used boundary condition (4.1) at $x = 0$ and $y = 0$. At $y = 16$ (the top) we set $u_h = u$ with u given by (5.1). Figure 2 shows the values of u_h and u at $x = 26$ when $\beta = 20$ and the outflow condition (4.8) is used at $x = 28$. The graph of u_h is marked with circles, and the graph of u is unmarked. We see that u_h has a wider boundary layer than u has. We see no oscillations. In fact, for computations with β as large as 2500 we saw no oscillations. The matrix equation for u_h was solved by the Yale Sparse Matrix Package [4, 5]. The Bessel function K_1 in (5.1) was evaluated by the algorithm of Russon and Blair [11].

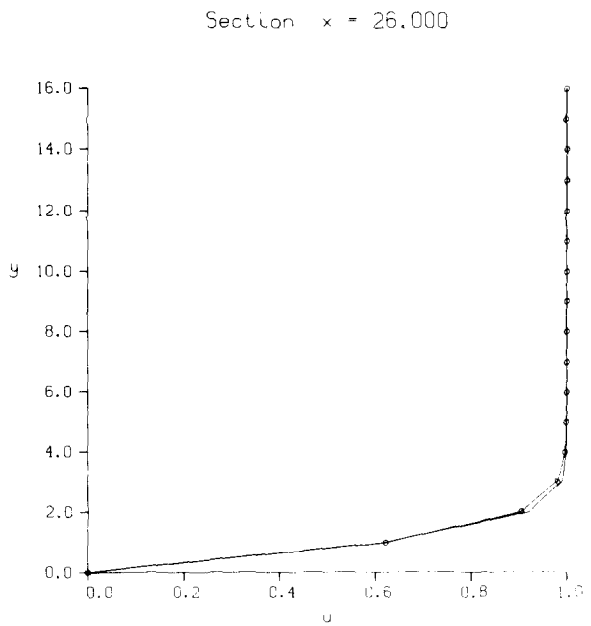

FIG. 2. Velocity profile under good outflow conditions.

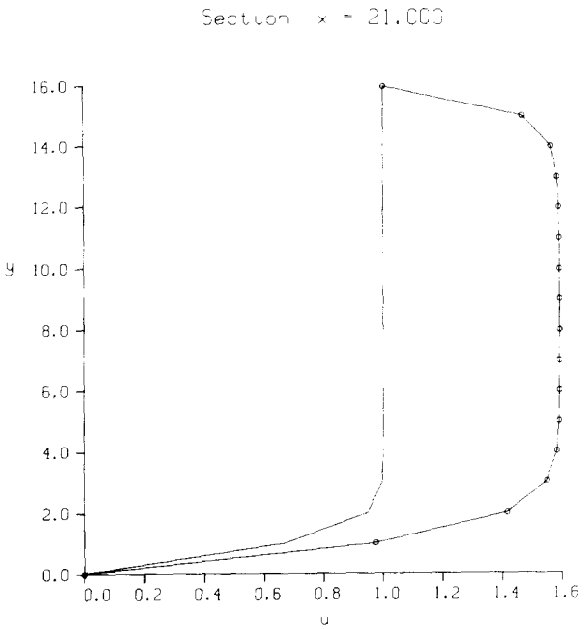

FIG. 3. Velocity profile under bad outflow conditions.

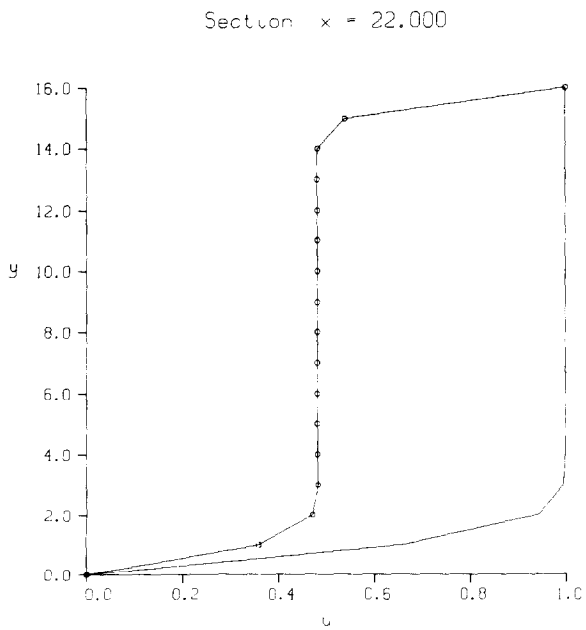

FIG. 4. Velocity profile under bad outflow conditions.

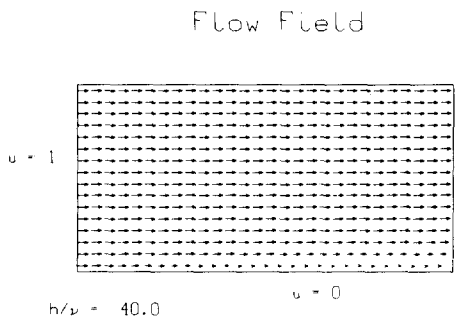

FIG. 5. Navier–Stokes with $h/\nu = 40$.

We also did computations with outflow boundary condition (4.9) in place of (4.8). These are not shown, because we found no significant difference.

Theorem 4.2 is illustrated in Figs. 3 and 4. We see the large oscillations caused by setting $u_h = 0$ at the outflow $x = 28$. Again, we are using $\beta = 20$. The boundary conditions at the other boundaries are as before, $u_h = u$ at $y = 16$ (the top) and (4.1) at $x = 0$ and $y = 0$. Note that the condition $u_h = u$ at the top produces a boundary layer there.

Finally, Fig. 5 shows the flow field obtained by solving the Navier–Stokes equations (1.9) using $\beta = 20$. The artificial compressibility method of Chorin [3] was used with central differences based on the stencil shown in Fig. 6. The boundary conditions used were $u = 1$ and $v = 0$ at $x = 0$, $u = 0$ and $v = 0$ at $y = 0$, $u_x = 0$ and $u_y = 0$ at $y = 16$ (the top), and discretizations of $uu_x = vu_{yy}$ and $v_y = -u_x$ at $x = 28$ (the outflow). We see again that the presence of a boundary layer parallel to the flow field does not produce numerical oscillations. A computation of the same problem with β changed to 250 gave essentially a uniform flow field outside a boundary layer of thickness h.

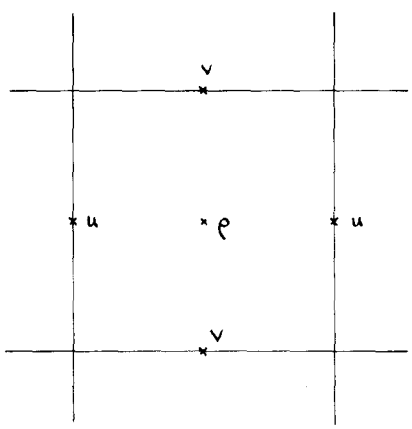

FIG. 6. The stencil.

6. Conclusions

We see that in a 2-dimensional computation the cell Reynolds number has two effects. First, there is the spurious component which is also observed in 1-dimensional problems. It gives grid-sized oscillations if the cell Reynolds number exceeds 2. This spurious component is greatly diminished by the use of proper outflow boundary conditions as described in Section 4. Second, there is the numerical viscosity which thickens the boundary layer in the computed solution. This is a much smaller effect, and we barely see it in Fig. 2, where the cell Reynolds number is 40.

APPENDIX: Mathematical Details

In this appendix we give some of the technical details in the proofs of the theorems. These details are applications of elementary complex analysis.

Notes on the proof of Theorem 2.1

The detail sloughed over in the proof in the text is the justification of the deformation of the path of integration from the real axis in the θ-plane in (2.1) to the real axis in the ξ-plane in (2.8) and then to the line $\operatorname{Im} \xi = A$. This point is resolved by an examination of the mapping (2.7). We break up (2.7) into the composition of the two mappings

$$v = \phi(\theta) = 1 + i\omega\theta - (1 + \theta^2)^{1/2}, \tag{A1}$$

$$v = -\xi^2/2 + iA\xi, \tag{A2}$$

with the branches chosen so that $v = 0$ and $\xi = 0$ when $\theta = 0$. For the mapping (A1) we take θ in the half-plane $\operatorname{Im} \theta > 0$, omitting a cut from i to $i\infty$ on the imaginary axis. It is easy to see that this region is mapped 1–1 onto a domain D in the ξ-plane. It also happens that symmetric points $(\theta, -\bar{\theta})$ with respect to the imaginary θ-axis are mapped into symmetric points $(\xi, -\bar{\xi})$ with respect to the imaginary ξ-axis. The justification for the movement of the path of integration from the real θ-axis to the real ξ-axis results from the fact that D contains the sectors bounded by the real ξ-axis and the image of the real θ-axis and from the fact that the image of the ray $0 < \theta < \infty$ is contained in the sector $|\arg \xi| < \pi/4$. Finally, the replacement of the real ξ-axis by the line $\operatorname{Im} \xi = A$ is justified because D contains the strip $0 < \operatorname{Im} \xi \leqslant A$.

Determination of c_0 *in* (2.10)

We begin by expanding ξ as a function of θ, based on (A1) and (A2),

$$\xi = iA + (1 + \omega^2)^{3/4}(\theta - \theta_0) + O(\theta - \theta_0)^2, \qquad \theta \to \theta_0.$$

Thus, we have

$$d\theta/d\xi|_{\xi=iA} = (1+\omega^2)^{-3/4},$$
$$c_0 = (g(iA)-1)/(iA) = -i(\omega^{-1}(1+\omega^2)^{-1/4} - A^{-1}).$$

This together with (2.10) gives (2.6).

Remark. We did the asymptotics by the method of van der Waerden [13] because that way we know we get an asymptotic series. Other ways to do it are as follows. Olver [9, pp. 344–351] replaces g in (2.8) by

$$g(\xi) = \sum_0^\infty d_j(\xi - iA)^j.$$

Bleistein [1] uses a Jacobi series [14, p. 57]

$$g(\xi) = \sum_0^\infty R_j \xi^j (\xi - iA)^j,$$

where each R_j is a first-degree polynomial in ξ. These methods are more appropriate when the singularity is a branch point. In both cases the formal expansion starts with the same error function as in (2.5), but subsequent terms are different.

Notes on the proof of Theorem 3.1

We begin by examining the function $r_1(\theta)$ defined by (3.4). We want to deform the path of integration in (3.6) into the complex plane, so we proceed to define a branch of $r_1(\theta)$. For $\beta \neq 1$ the function $r_1(\theta)$ has two branch points in the half-strip $|\operatorname{Re}\theta| \leqslant \pi$, $\operatorname{Im}\theta \leqslant 0$, located at the roots of

$$s^2 = (2-\cos\theta)^2 = 1-\beta^2. \tag{A3}$$

If $0 < \beta < 1$, these branch points lie on the imaginary axis, and we connect them with a cut on the imaginary axis. If $\beta > 1$, the branch points are symmetric with respect to the imaginary axis. We then make cuts in the θ-plane in such a way that the images of the cuts in the s-plane under (3.3) are lines from $(\beta^2-1)^{1/2}$ to $i\infty$ and from $-i(\beta^2-1)^{1/2}$ to $-i\infty$. See Figs. 1 and 7. Thus, we have a domain Ω in the θ-plane on which the function $r_1(\theta)$ is analytic. The image of Ω in the r_1-plane is the half-plane $\operatorname{Re} r_1 > 0$, minus a cut on the real axis arising from the interval $-\pi \leqslant \theta \leqslant \pi$.

A note on the saddle points of ϕ_h in Ω

If $\beta \leqslant 1$ or $\omega \leqslant 1$, then (3.9) and (3.3) give the only saddle point in Ω. However, if $\beta > 1$ and $\omega > 1$, then there are two saddle points in Ω, the second one obtained by changing the sign of the square root in (3.9). Furthermore, these two saddle points coalesce at the value of θ given by (3.3) and $s_0 = 2/(1-\omega_1^2)$, if $\omega \to \omega_1$ with ω_1 given by

$$\beta\omega_1(\omega_1^2-1)^{1/2} = \omega_1^2 + 1. \tag{A4}$$

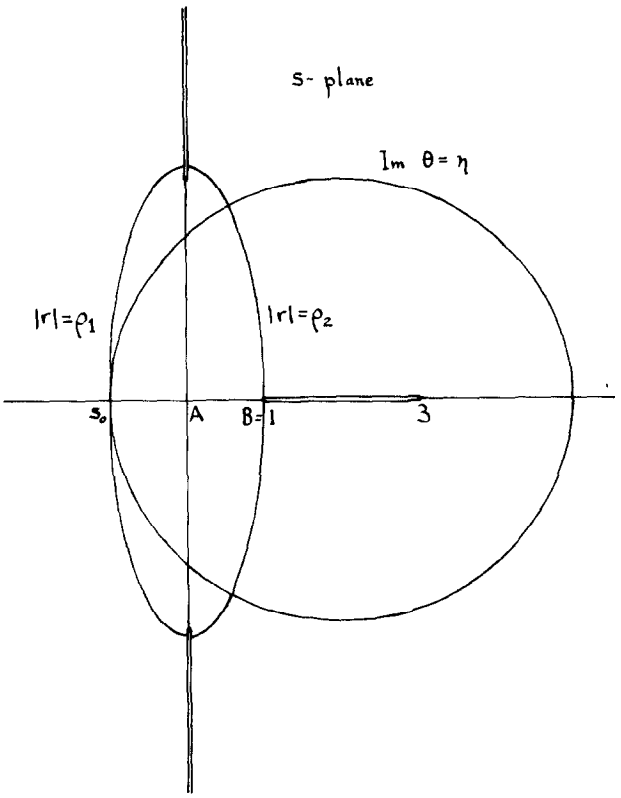

FIG. 7. s-plane.

It is clear that (A4) defines β as a decreasing function of ω_1 for $1 < \omega_1 < \infty$. Hence, given $\beta > 1$, Eq. (A4) has a unique solution ω_1. For $\omega > \omega_1$ the two saddle points are symmetric with respect to the imaginary axis, and the elevation $\mathrm{Re}\,\phi_h(\theta_0)$ is the same for both of them. Furthermore, as $\omega \to \infty$, the saddle points tend to the branch points.

Lemmas on the topography in Ω

We now present two lemmas which provide information about hills, valleys, and branch cuts to enable us to construct a good path of integration.

LEMMA A1. *For θ in Ω let $\phi_h(\theta)$ be as defined in* (3.7). *Let $0 < \beta_0 \leqslant \beta$ for some positive β_0. If $\beta > 1$, let $\omega < \omega_1$, where ω_1 is the solution of* (A4). *Then for the saddle point θ_0 given by* (3.9) *we have*

$$\phi_h''(\theta_0) < 0. \tag{A5}$$

Proof. A direct calculation shows that

$$\phi_h''(\theta) = (s-2)(\beta^2 + s^2 - 1)^{-1/2} - s((2-s)^2 - 1)(\beta^2 + s^2 - 1)^{-3/2}$$

with s as in (3.3). Hence, $\phi_h''(i\eta)$ is real for real η. Thus, if $\theta = i\eta$ is such that

$$1 - \beta^2/4 - (\beta/4)(\beta^2 + 8)^{1/2} < s \leqslant 1, \tag{A6}$$

we see that $\phi_h''(\theta) < 0$. For $\beta > 1$ and $\theta = \theta_0$ the restriction $0 \leqslant \omega < \omega_1$ of the lemma is equivalent to (A6). For $0 < \beta \leqslant 1$ and $\theta = \theta_0$ th restriction (A6) is automatic because $(1-\beta^2)^{1/2} < s_0 \leqslant 1$ if $s_0 = 2 - \cos\theta_0$. This proves the lemma.

LEMMA A2. *For $\beta > 1$ let θ_b be the branch point θ given by* (A3) *with* $\operatorname{Re}\theta_b > 0$. *Let $0 \leqslant \eta < \infty$ if $\beta_0 \leqslant \beta \leqslant 1$ and let $0 \leqslant \eta \leqslant \operatorname{Im}\theta_b$ if $\beta > 1$. Then on the segment*

$$\gamma_\eta = \{\theta: \operatorname{Im}\theta = \eta,\ -\pi \leqslant \operatorname{Re}\theta \leqslant \pi\} \tag{A7}$$

$\operatorname{Re}\phi_h(\theta)$ *has its maximum at $\theta = i\eta$ and nowhere else on γ_η. Furthermore, there exists a positive function $P(\beta)$, bounded away from zero, such that* $\operatorname{Im}\theta_0 \leqslant \operatorname{Im}\theta_b$ *for the saddle point θ_0 of* (3.9) *if $0 \leqslant \omega < P(\beta)$ and $0 < \beta < \infty$.*

Remark. The conclusion $P(\beta) \geqslant \omega_2 > 0$ is important in that the lemma implies that we may use the saddle-point method for $0 < \beta_0 \leqslant \beta < \infty$ and $0 \leqslant \omega \leqslant \omega_2$. This is significant since the region $0 \leqslant \omega \leqslant \omega_2$ contains the boundary layer.

Proof. For fixed ω let us examine the value on γ_η of

$$\begin{aligned} \operatorname{Re}\phi_h(\theta) &= \log|r| - \omega\eta, \\ r &= (-s + (s^2 + \beta^2 - 1)^{1/2})/(\beta - 1), \\ s &= 2 - \cos\theta. \end{aligned} \tag{A8}$$

It is clearly sufficient to consider the images in the s-plane of γ_η and of the semicircles $|r| = \rho$ with $\operatorname{Re} r \geqslant 0$. (Recall that our definition of the branch cuts was such that $\operatorname{Re} r \geqslant 0$ for θ in Ω.) In terms of $s = \sigma + i\tau$ the image of γ_η is the ellipse

$$(\sigma - 2)^2/\cosh^2\eta + \tau^2/\sinh^2\eta = 1 \tag{A9}$$

with foci at $s = 1, 3$.

We now determine the image in the s-plane of $|r| = \rho$, $\operatorname{Re} r > 0$, under the inverse image of (A8),

$$s = (\beta + 1)/(2r) - (\beta - 1)r/2.$$

We concentrate on the case $\beta > 1$ because the argument is more delicate then. The special half-circle

$$|r| = \rho_0 = (\beta + 1)^{1/2}(\beta - 1)^{1/2}, \qquad \operatorname{Re} r > 0,$$

is mapped onto the segment joining the branch points

$$s_b = \pm i(\beta^2 - 1)^{1/2}. \tag{A10}$$

For other values of ρ the image of $|r| = \rho$, $\operatorname{Re} r > 0$, is a half-ellipse in the s-plane with foci at the branch points (A10),

$$\begin{aligned} \sigma^2/b^2 + \tau^2/a^2 &= 1, \\ b &= |\beta + 1 - (\beta - 1)\rho^2|/(2\rho), \\ a &= (b^2 + \beta^2 - 1)^{1/2}. \end{aligned} \tag{A11}$$

See Fig. 7. If $0 < \rho < \rho_0$ the half-ellipse (A11) is in the half-plane $\operatorname{Re} s > 0$. For $\rho > \rho_0$ it is in the half plane $\operatorname{Re} s < 0$. Furthermore, as ρ increases, the half ellipses in the s-plane move to the left monotonically.

With this geometric background we are able to determine the behavior of $\operatorname{Re} \phi_h(\theta)$ for θ on γ_η. First, if η is so small that the ellipse (A9) is contained in the half-plane $\operatorname{Re} s \geqslant 0$, it is clear that $\operatorname{Re} \phi_h(\theta)$ has its maximum on γ_η at $\theta = i$. (This is what happens for $0 < \eta < \infty$ if $0 < \beta \leqslant 1$. Thus, we have $P(\beta) = \infty$ for $0 < \beta \leqslant 1$.) Second, consider an ellipse (A9) with σ-intercept $-b$ with $b > 0$ and with the condition that the ellipse misses the cuts. That is, we require that on the ellipse (A9) we have $\tau^2 \leqslant \beta^2 - 1$ when $\sigma = 0$. One such ellipse is shown in Fig. 7. A direct calculation shows that these conditions are equivalent to

$$(2 + b)^2 \leqslant (\beta^2 + 4 + \beta(\beta^2 + 8)^{1/2})/2. \tag{A12}$$

On the curve γ_η corresponding to an ellipse of this sort $\operatorname{Re} \phi_h(\theta)$ has its maximum at $\theta = i\eta$ if and only if the ellipses (A9) and (A11) through the point $(\sigma, \tau) = (-b, 0)$ have no other intersection in the half plane $\sigma < 0$. But, by eliminating τ^2 from (A9) and (A11) we obtain a quadratic for σ, so that ellipses (A9) and (A11) intersect for at most two values of σ. Because the foci for ellipses (A11) lie outside of the ellipses (A9) under consideration and because the ellipses meet at $(\sigma, \tau) = (-b, 0)$, it is clear that there are two other intersections for some positive value of σ. See Fig. 7. (This agrument also shows that the ellipses (A9) and (A11) do not osculate at $s = -b$.) Thus, if (A12) holds, we see that the ellipse (A9) through $s = -b$ is to the right of the half-ellipse (A11) through $s = -b$. This shows that on γ_η the function $\operatorname{Re} \phi_h(\theta)$ has its maximum at $\theta = i\eta$ and nowhere else.

It remains to determine $P(\beta)$, that is, we need to know the restrictions on ω under which the saddle points θ_0 maps into $s_0 = -b$ for positive b satisfying (A12). For $0 \leqslant \omega \leqslant \omega_1$ with ω_1 given by (A4), Eq. (3.9) defines s_0 as a decreasing real function of ω. Thus, the inverse function of (3.9) together with

$$(2 - s_0)^2 = (\beta^2 + 4 + \beta(\beta^2 + 8)^{1/2})/2 \tag{A13}$$

determines a continuous function $P(\beta)$ for $\beta > 1$ such that $\gamma_\eta \subset \Omega$ if $0 \leqslant \omega < P(\beta)$ and $\eta = \operatorname{Im} \theta_0$. (We have already seen that the ellipses (A9) and (A11) do not osculate at

s_0 if $0 \leqslant \omega \leqslant P(\beta)$. It is easy to verify that these ellipses do osculate at s_0 if $\omega = \omega_1$. Thus, it follows that $P(\beta) < \omega_1$.)

Finally, we show that $P(\beta)$ is bounded away from zero. Since $0 \leqslant s_0 < 1$ for ω small enough, it is clear that $P(\beta) > 0$ for $1 < \beta < \infty$. Thus, in order to prove that $P(\beta)$ has a positive lower bound, it suffices to examine the behavior of $P(\beta)$ as $\beta \to 1$ and $\beta \to \infty$. An examination of (3.9) and (A13) shows that

$$\lim_{\beta \to 1} P(\beta) = \infty, \qquad \lim_{\beta \to \infty} P(\beta) = 2^{-1/2}.$$

Thus, we see that $P(\beta)$ has a positive lower bound, and this completes the proof of the lemma.

The behavior of u_h for $\beta > 1$ and $\omega > P(\beta)$

We now obtain a crude estimate of $|u_h - 1|$ in the region near the inlet, $\omega > P(\beta)$, when $\beta > 1$. Lemmas A1 and A2 show that for $\beta > 1$ and $\omega > P(\beta)$ we may integrate (3.6) along a line through the branch points, $\eta = \operatorname{Im} \theta_b$, and obtain the estimate

$$|u_h - 1| \leqslant C \int_{\gamma_\eta} \exp\{n \operatorname{Re} \phi_h\}\, d\theta.$$

If $\omega = P(\beta)$, then $\theta_0 = i\eta$ is the saddle point (3.9). Also, if $\omega > P(\beta)$, then on γ_η we have

$$\operatorname{Re} \phi_h(\theta, \omega) = \operatorname{Re} \phi_h(\theta, P(\beta)) - \eta(\omega - P(\beta)).$$

(Here, we make explicit the dependence of ϕ_h on both θ and ω.) Thus, using Lemmas A1 and A2, for $\beta > 1$ and $\omega > P(\beta)$ we obtain

$$|u_h - 1| \leqslant C' n^{-1/2} \exp\{n\phi_h(i\eta, P(\beta)) - n\eta(\omega - P(\beta))\}, \tag{A14}$$

with $\phi_h(i\eta, P(\beta)) < 0$. Consequently, $|u_h - 1|$ is even smaller for $\omega > P(\beta)$ than it is for $\omega = P(\beta)$.

ACKNOWLEDGMENTS

The authors would like to thank R. C. Y. Chin and Joseph Oliger for their helpful comments.

REFERENCES

1. N. BLEISTEIN, *Comm. Pure Appl. Math.* **19** (1966), 353.
2. J. H. BRAMBLE, B. E. HUBBARD, AND V. THOMÉE, *Math. Comp.* **23** (1969), 695.
3. A. J. CHORIN, *J. Comput. Phys.* **2** (1967), 12.
4. S. C. EISENSTAT, M. C. GURSKY, M. H. SCHULTZ, AND A. H. SHERMAN, Research Report #112, Department of Computer Science, Yale University, 1977.

5. S. C. EISENSTAT, M. C. GURSKY, M. H. SCHULTZ, AND A. H. SHERMAN, Research Report #114, Department of Computer Science, Yale University, 1977.
6. B. ENGQUIST AND A. MAJDA, *Math. Comp.* **31** (1977), 629.
7. A. ERDÉLYI, "Tables of Integral Transforms," Vol. 1, McGraw-Hill, New York, 1954.
8. N. LEVINSON, *Ann. of Math.* **51** (1950), 428.
9. F. W. J. OLVER, "Asymptotics and Special Functions," Academic Press, New York, 1974.
10. P. J. ROACHE, "Computational Fluid Dynamics," Hermosa, Albuquerque, 1972.
11. A. E. RUSSON AND J. M. BLAIR, Report AECL-3461, Atomic Energy of Canada Limited, Chalk River, Ontario, 1969.
12. M. SAPAGOVAS AND R. SKIRMANTAS, *Differencial'nye Uravnenija* **17** (1977), 75.
13. B. L. VAN DER WAERDEN, *Appl. Sci. Res. Ser. B* **2** (1951), 33.
14. J. L. WALSH, "Interpolation and Approximations by Rational Functions in the Complex Domain," Edwards, Ann Arbor, Mich., 1956.